Results of steel specimens tensile testing using the metal magnetic memory method

Anatoly A Dubov
Energodiagnostika Co. Ltd., Russia, mail@energodiagnostika.ru

Abstract

It is known that the main sources of damages occurrence in operated engineering products and structures are stress concentration zones (SCZs), in which metal corrosion, fatigue and creep processes develop most intensively. Sizes of local SCZs, in which the metal reaches failure stress with formation of micro- and macrocracks, range from several micrometers to several millimeters. In recent years the metal magnetic memory (MMM) method becomes more and more widespread in practical application in Russia and a number of other countries. The MMM method – is a passive non-destructive testing method based on the analysis of self-magnetic leakage fields (SMLF) distribution on the products' surface to detect SCZs, defects and structural inhomogeneities of the metal in products and welded joints. The MMM method does not require external magnetization or any preparation of products' surfaces to carry out the inspection. One of the main tasks of the MMM method is detection of local SCZs on the surface and in deep layers of the metal of various inspection objects (IO), as well as determination of the metal's limit strain state before its failure. Tensile tests of specimens made of steel 20 with simultaneous measurement of magnetic and mechanical parameters were carried out. Correlation between variation of the specimens' self-magnetic leakage field and their deformation was demonstrated. Relation between magnetic and mechanical parameters, characterizing the limiting strain capacity of the metal, was established. The possibility of the metal magnetic memory method application to determine the true limit failure stress was demonstrated.

1. Introduction

It is known that the main sources of damages occurrence in operated engineering products and structures are stress concentration zones, in which metal corrosion, fatigue and creep processes develop most intensively. Sizes of local SCZs, in which the metal reaches failure stress with formation of micro- and macrocracks, range from several micrometers to several millimeters. In recent years the metal magnetic memory (MMM) method becomes more and more widespread in practical application in Russia and a number of other countries. One of the main tasks of the MMM method is detection of local SCZs on the surface and in deep layers of the metal of various inspection objects (IO), as well as determination of the metal's limit strain state before its failure.

According to (1), the MMM method – is a passive non-destructive testing method based on the analysis of self-magnetic leakage fields distribution on the products' surface to detect SCZs, defects and structural inhomogeneities of the metal in products and welded joints. The MMM method does not require external magnetization or any preparation of

products' surfaces to carry out the inspection. Special magnetometric instruments in combination with multi-channel devices are used during the inspection of products.

Papers (2, 3, 4) found that magnetic anomalies occur under the impact of workloads in local SCZs of products due to magnetomechanical effects. Detection of such magnetic anomalies makes it possible to find SCZs and to assess the degree of their hazard. The recorded parameters of SMLF are the value and direction of the magnetic field induction/intensity vector and the magnetic field induction/intensity gradient.

According to (1), one of the basic diagnostic parameters in the MMM method is the design parameter *m* that characterizes the metal's strain capability and allows to quantitatively determine the moment of a macrocrack formation in the local SCZ of equipment and structures.

2. Formulation of a task

When calculating strength of various equipment elements and components, the yield strength (R_e) and tensile strength (R_m) are accepted as basic mechanical characteristics of the metal. They are conventional, as they are determined under accepted conditions of testing of specimens with conventionally accepted dimensions. Studies (3, 5) found that actual values of limiting mechanical characteristics for materials embodied in specific product shapes may differ significantly from the reference ones due to the scale factor and other conditions of objects loading. It was shown that mechanical characteristics R_e and R_m are only conventional equivalents of internal stresses due to the external effect, and in order to judge about variation of the material's internal energy or internal stresses, it is necessary to use other characteristics of the material's reaction to this effect as well, in particular, the longitudinal and transverse strain. Especially since strain of both specimens and real objects is measurable.

As it is known, the physical basis of strain processes in metals is the glide of dislocations and their accumulation in SCZs of products. It should be noted here that SCZs are not only pre-known areas where the design features create different conditions for distribution of stresses caused by an external load, but these are also randomly located areas, in which due to the initial metal heterogeneity combined with off-design additional workloads large strains (as a rule, shear strains) occur.

Papers (2, 3) demonstrated that when the strain energy is by an order of magnitude more than the energy of a weak external magnetic field in areas of maximum strain and dislocation clusters, there occur self-magnetic leakage fields, the size and direction of which reflect the strain tensor.

One of the basic calculation diagnostic parameters the MMM methods uses the parameter *m* that characterizes the strain capability of the metal. The standard on the MMM method (6) provides the definition of the parameter *m:*

$$m = \frac{K_{in}^{max}}{K_{in}^{ave}}, \quad (1)$$

where K_{in}^{max} and K_{in}^{ave} are, respectively, the maximum and the average factors of the magnetic field H variation intensity or their gradients $|\Delta H|$ on the length Δx between two adjacent points, which are determined in SCZs of products during their inspection.

It was indicated (6) that if the parameter m exceeds the limiting value m_{lim}, which is determined in laboratory and industrial conditions, then a conclusion is drawn about the limiting state of the metal preceding damaging of IO. The physical meaning of this parameter for the ratio of mechanical characteristics is revealed in paper (3).

To establish correlation between the magnetic and mechanical characteristics of steel 20, tensile tests of flat specimens with simultaneous measurement of the specimens' SMLF by the MMM method were carried out at Fraunhofer Institute IZFP, Saarbrucken.

3. Results of tensile tests of specimens

Tests were carried out on 3 specimens of steel 20 using the ZWICK ROELL Z050 tensile testing machine. Chemical composition of steel 20 is given in Table 1. Mechanical properties of steel 20 in accordance with GOST 4041-71: R_m = 340-490 MPa, ε = 22-28 %.

Table 1. Chemical composition of steel 20

Chemical element	*C*	*Si*	*Mn*	*Ni*	*P*	*S*	*Cu*	*Cr*
Content [wt.%]	0.169	0.212	0.357	0.035	0.0015	0.002	0.069	0.047

Geometrical dimensions of the specimens with the gauge length cross section of 12.05x1.73 mm are shown in Figure 1. Mounting locations of three-component sensors (4 pcs.) for SMLF measuring on the work surface of the specimen during its tension are indicated with symbols (+).

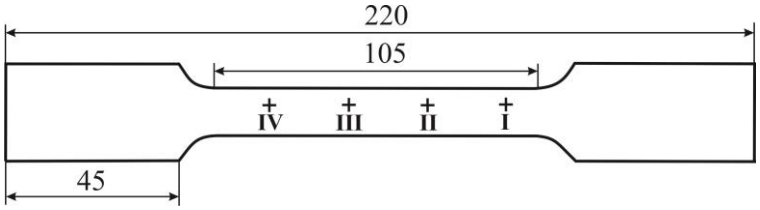

Figure 1. Geometrical dimensions of specimens, mm

Sensors were mounted in close proximity to the specimen's surface (about 0.5 mm) equally spaced (about 15 mm) with total displacement towards the moving clamp of the tensile testing machine (Figure 2). Sensors were connected to the TSC-7M-16 type magnetometer manufactured by Energodiagnostika Co. Ltd. (Moscow).

After placing the specimen into the tensile testing machine clamps, the TSC-7M-16 instrument switched on, and measurements of the specimen's SMLF right up to its failure were performed in the "timer" mode with simultaneous application of tensile load at a strain rate of 2 mm/min.

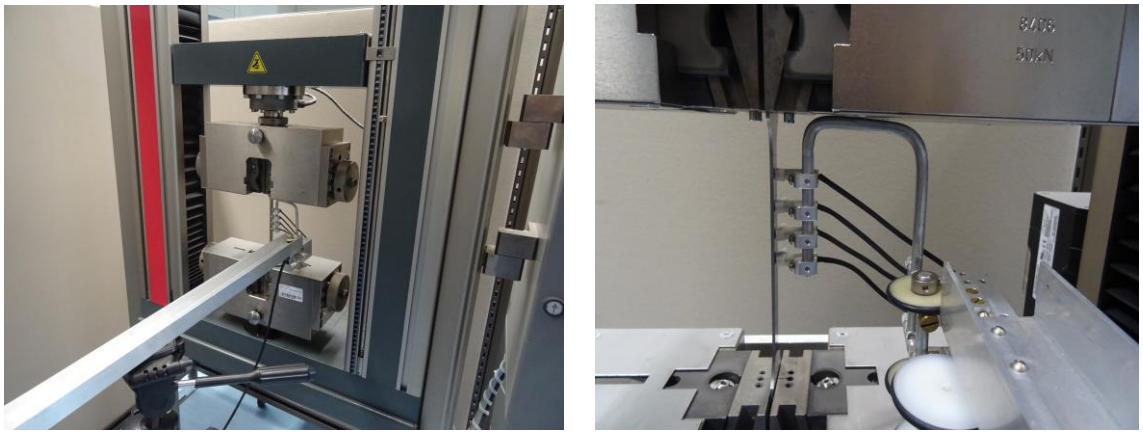

Figure 2. Relative position of the specimen and sensors during measurements

Processing of SMLF measurement results depending on the strain time and value, recorded on the tensile testing machine diagram, was carried out using the special "MMM-System" program after the recorded data transfer from the TSC-7M-16 instrument to the personal computer. At the same time the program automatically calculated the resultant magnetic field value at each point of SMLF measurement using the algorithm:

$$H = \sqrt{H_x^2 + H_y^2 + H_z^2}\ . \tag{2}$$

Figure 3, *a* shows the graph of variation of the resultant magnetic field *H* depending on the specimen relative elongation ε at the point closest to the specimen *3* rupture location. The tensile diagram σ - ε of specimen *3* is shown in Figure 3, *b*. Points *A, B, C, D, E, G, K* in Figure 3, *a* indicate:

A – magnetic field *H* value in the initial state (load *F*=0);
B – field *H* value after reaching the proportional limit;
C – field *H* value at the yield strength R_e at yield drop;
D – maximum field *H* value at yield point;
E – field *H* value in the uniform strain area;
G – field *H* value after reaching the tensile strength R_m of the specimen;
K – field *H* value at the specimen rupture;
R_w – is the true tensile strength of the specimen's material, calculated as the ratio of the applied force at the time of the specimen failure to the specimen's neck cross-sectional area measured after this specimen failure.

Based on the obtained data, the magnetic value of strain capacity *m* used in the MMM method in accordance with ISO 24497-2:2007(E) (1) was estimated:

$$m = \frac{\sum|\Delta H_w|}{\sum|\Delta H_m|} \approx \frac{R_w}{R_m}, \tag{3}$$

where $\sum|\Delta H_w|$ and $\sum|\Delta H_m|$ – are total values of modular variations of the field *H* intensity from the beginning of load application (point *A* in Figure 3, *a*) to the moment of reaching the true tensile strength (point *K* in Figure 3, *a*) or to the tensile strength point *G*, respectively.

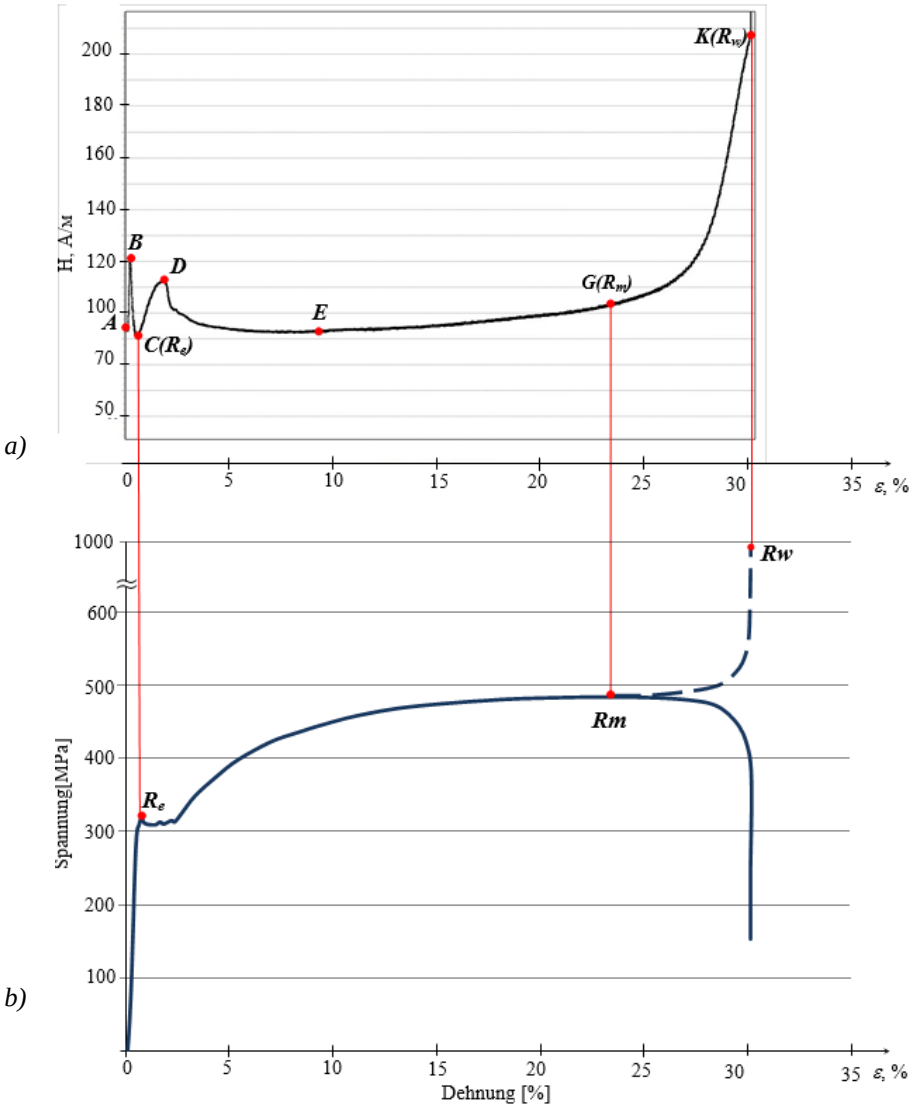

Figure 3. Graph of variation of the resultant magnetic field *H*, being closest to the rupture location for specimen *3* (*a*) and the tensile diagram σ - ε of specimen *3* (*b*)

Calculations of these values are performed by the field *H* values in characteristic points *A, B, C, D, E, G, K* using the relations:

$$\sum|\Delta H_m| = |\Delta H_{AB}| + |\Delta H_{BC}| + |\Delta H_{CD}| + |\Delta H_{DE}| + |\Delta H_{EG}|, \qquad (4)$$
$$\sum|\Delta H_w| = |\Delta H_{GK}| + \sum|\Delta H_m|.$$

Substituting in the above ratio (4) numerical values of $\sum|\Delta H_w|$ and $\sum|\Delta H_m|$, we obtain the following for the specimen *3*:

$$\sum|\Delta H_m| = |\Delta H_{AB}| + |\Delta H_{BC}| + |\Delta H_{CD}| + |\Delta H_{DE}| + |\Delta H_{EG}| = 26+30+22+20+8 = 106 \text{ A/m},$$
$$\sum|\Delta H_w| = |\Delta H_{GK}| + \sum|\Delta H_m| = 108 + 106 = 214 \text{ A/m}.$$
$$m = \frac{214}{106} \approx 2{,}02.$$

The tensile strength of the specimen material R_w was calculated by the relation:

$$R_w = \frac{F_{Bruch}}{A_{Bruch}}, \quad (5)$$

where F_{Bruch} – is the tensile force applied to the specimen at the time of its rupture, A_{Bruch} – the specimen's cross section at the point of rupture.

$$R_w = \frac{81078.4\text{Newton}}{8.16\text{mm}^2} \approx 990\text{MPa}.$$

Then, based on the measurements on specimen *3*, the relation of the true tensile strength R_w to the tensile strength R_m of steel 20 will be $R_w/R_m = 990/480 \approx 2.06$, which is close to the magnetic parameter value $m = 2.02$.

Magnetic and mechanical values obtained during testing of specimens *1* and *2* (see Table 2) were calculated similarly using the relation (3), (4) and (5). Table 2 shows that the values of the magnetic parameter m and the ratio R_w/R_m practically equal. The maximum difference between the numerical values of these parameters was obtained for specimen *1*, on which location of the field measuring sensor turned out to be displaced by about 10 mm from the specimen rupture point. On specimens *2* and *3* the locations of one of the field H measuring sensors practically coincided with the specimens rupture points, therefore the difference between the magnetic and the mechanical parameter m was negligible.

Table 2. Magnetic and mechanical values for three specimens of steel 20

Specimen No.	R_m, MPa	F_{Bruch}, N	R_w, MPa	A_0, mm^2	A_{Bruch}, mm^2	$\Sigma\lvert\Delta H_w\rvert$, A/m	$\Sigma\lvert\Delta H_m\rvert$, A/m	Parameter m	R_w/R_m
1	460	7816.5	965	20.85	8.1	218	97	1.9±0.19	2.09
2	460	7750.3	1087	20.4	7.13	243	99	2.45±0.09	2.36
3	480	8078.4	990	20.85	8.16	214	106	2.02±0.12	2.06

4. Discussion of results

Determination of the relation R_w/R_m based on mechanical characteristics should not cause any doubts, as the values of F_{Bruch} were recorded on the tensile testing machine in the course of standard tests, and cross-sectional area of specimens A_{Bruch} at the point of failure was calculated based on the section photograph at magnification x10, and its subsequent transfer on the graph paper. However, for the values of the parameter m obtained using the relations (3) and (4) based on the measured values of the resultant magnetic field H and its gradient $|\Delta H|$, it is necessary to provide some clarification.

Let us consider in more detail the variation curve of the self-magnetic field H of specimen *3* versus the diagram σ - ε (Figure 3, *b*). Diagram H - ε shows that on the length from the point A (initial state at the tensile force F=0) to the point B the field H increases reaching its maximum at the point B, and after the point B the field H decreases to the point C that corresponds to the initial yield drop point on the diagram σ - ε. Further the field H increases noticeably from the point C to the point D – transfer from Chernov-Luders bands formation area to the uniform strain area. To calculate the

stress level σ, corresponding to the point *B* on the field *H* curve, let us use the following fact. On the diagram σ - ε length from 0 to the beginning of the yield area stress σ is close to the linear law of variation from ε (Hooke's law). Tensile testing of specimens was performed at a constant tensile rate of 2 mm/min. The time interval of single magnetic field measurement with sensors is a constant, which allows to estimate the position of the point *B* on the diagram σ - ε.

Figure 4 shows the distribution of the magnetic field *H* recorded on specimen *3* in the "timer" mode on the length from the beginning of load application to the yield point yield point depending on the number of measurements *n*. X-axis (abscissa) may also be represented in measuring time units through multiplying the number of measurement by a single measurement time interval.

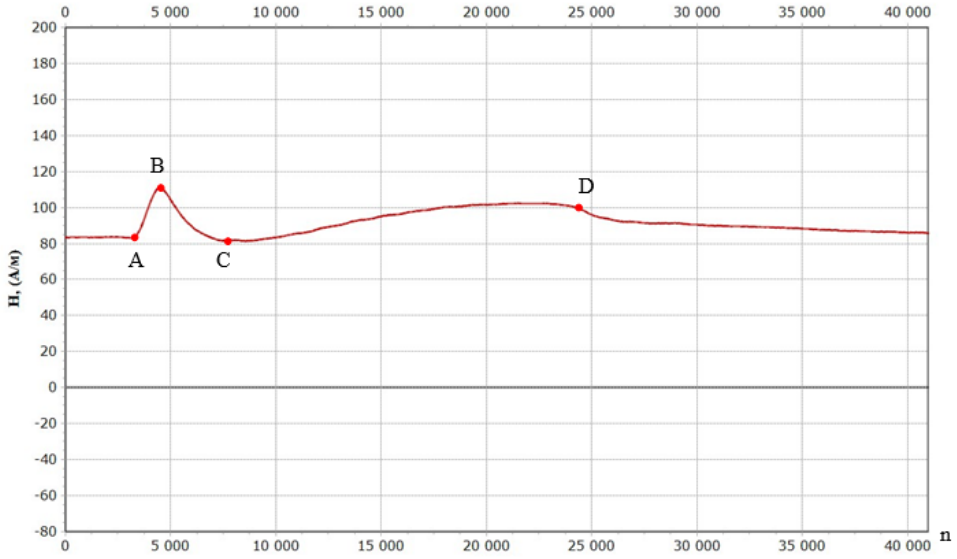

Figure 4. Distribution of the magnetic field *H* recorded on specimen *3* in the "timer" mode on the length from the beginning of load application to the yield point yield point depending on the number of measurements *n*

It follows from Figure 4 that at the point *B* the number of field *H* measurements, recorded in the "timer" mode using the TSC-7M-16 instrument, is about 1150, and at the point *C*, corresponding by the specimen strain time to the yield strength (R_e ~ 330 MPa), the number of measurements is about 3850. Then, taking into account the variation linearity of $\sigma(\varepsilon)$ and $n(t)$, we obtain the stress level corresponding to the point *B*:

$$\frac{1150}{3850} \times 330\text{MPa} = 98.6 \text{ MPa } (\approx 0{,}3R_e). \qquad (6)$$

It should be noted that on the other two tested specimens *1* and *2* characteristic changes of the field *H* were obtained on the length *AB* with clear record of its variation at the point *B*. At that, based on calculation using the relation (6), using the same time characteristics of tests on the diagram σ - ε and the field *H* curve, on specimens *1* and *2* the values of σ at the point *B* were obtained, which were also equal to about $0.3R_e$. We relate the found stress value at the point *B* to the proportional limit R_E.

According to (2, 3), the specimen's measured self-magnetic field *H* reflects the energy of resistance to straining, and the area of recorded inflection on the field *H* curve (point *B*) corresponds to the minimum of the internal energy spent by the material for resistance to the change of the glide plane inclination. The length *AB* on the curve *H* reflects the maximum variation of the initial glide planes arrangement in the specimen. On this length the main direction of glide planes is formed in the specimen under the effect of the applied load. The energy of resistance to straining of the considered specimen *3* under the load of 98.6 MPa (point *B* on the curve *H*) tends to a minimum due to the formation of the main direction of glide.

Point *B* corresponds to the boundary, after which the energy of resistance to elastic longitudinal strain becomes less than the plastic strain energy. At the same time the glide planes rotation angle relative to the external load direction begins to increase, which contributes to the increase of longitudinal plastic strain.

5. Conclusions

5.1 Based on the performed tensile tests of steel specimens using ZWICK ROELL Z050 tensile testing machine with simultaneous measuring the specimens' SMLF by the MMM method, correlation between SMLF variations and strain was established.

5.2 It was demonstrated that the magnetic diagnostic parameter *m* for all three tested tensile specimens turned out to be practically equal to the relation of mechanical characteristics R_w/R_m.

5.3 Application of the metal magnetic memory method allows to assess the limiting strain capacity of the metal and the true limit failure stress, as well as the proportional limit of ferromagnetic steels.

5.4 The results of carried out tests of specimens indicate the possibility in principle to use the MMM method in assessment of ferromagnetic steel products' stress-strain state.

References and footnotes

1. ISO 24497-1:2007(E) Non-destructive testing - Metal magnetic memory - Part 1: Vocabulary.
2. VT Vlasov, AA Dubov, "Physical bases of the metal magnetic memory method", Moscow: ZAO "Tisso", 2004, 424 p.
3. VT Vlasov, AA Dubov, "Physical theory of the "strain - failure" process - Part I: Physical criteria of the metal's limiting states", Moscow: ZAO "Tisso", 2007, 517 p.
4. AA Dubov, AlA Dubov, SM Kolokolnikov, "The metal magnetic memory method and inspection instruments: Training handbook", Moscow: "Spectr" Publishing House, 2012, 395 p.
5. VT Vlasov, AA Dubov, "Physical theory of the "strain - failure" process - Part II: Process thermodynamics", Moscow: "Spectr" Publishing House, 2016, 228 p.
6. ISO 24497-2:2007(E) Non-destructive testing - Metal magnetic memory - Part 2: General requirements.